Tina Memo No. 2001-002
Short Version published in:
Physiological Measurement, 20, 251-263, 1999.

The Effects of Motion on Parametric fMRI Analysis Techniques.

N.A.Thacker, E. Burton, A.J.Lacey and A.Jackson.

Last updated
3 / 5 / 1999

Imaging Science and Biomedical Engineering Division,
Medical School, University of Manchester,
Stopford Building, Oxford Road,
Manchester, M13 9PT.

1 Abstract

Subject motion during the time course of functional activation studies has been shown to cause spurious signals which can mimic "true" activation. Therefore, the importance of motion correction has been widely recognised. Correction with navigator echoes or post-processing using image registration software are common practice in functional imaging and analysis. Many image registration algorithms, developed for analysis requirements other than fMRI, assume rigid body motion. Although these techniques are now routinely used by a number of groups, rigid body co-registration has not yet been shown to reduce the effects of motion to an acceptable level in fMRI analysis ie: the effects on resulting correlation analysis directly. In this paper we have used volume data to assess rigid body coregistration in terms of motion artefacts for the different correlation approaches used in fMRI. We have developed a new way of visualising motion effects in correlation analysis based on generating a scatter plot of correlation score vs local image gradient. This technique has been tested on fmri data sets from a functional paradigm sufferening from motion correlated artefacts, with and without rigid body motion correction. Although we do not attempt to estimate the actual residual motion, this technique can be used to varify the results of analysis and select regions of relatively unambiguous activation. This paper assesses directly the rigid body assumption and proves the need for, and effectiveness of co-registration, for all correlation based analysis techniques. The specific differences between the popular correlation forms used are investigated and explained. We show that for certain forms of correlation analysis the effects of motion, while not removed altogether, are effectively statistically eliminated.

Key Words: BOLD, image analysis, motion, artefact.

2 Introduction

The importance of motion correction in Functional Magnetic Resonance Imaging (fMRI) has been widely recognised in the literature [9]. There seems to be a standard approach emerging to the problem in clinical environments making use of software available on the internet, such as the Automatic Image Registration package (AIR) [17, 18, 10] which assumes a rigid body motion. Many groups, now routinely make use of rigid body co-registration though it has not (to our knowledge) been proven that the effects caused by motion are reduced to an acceptable level in the subsequent fMRI analysis. Depending upon the details of the data acquisition, a rigid body assumption may be considered a little naive depending on the sequence employed. In some cases slices of image data may undergo different amounts of motion and in other cases the data may suffer from motion blurring. These processes could leave residual motion artefacts in the data which bias subsequent interpretation.

Previous workers have demonstrated the potential problems of motion in fMRI analysis [9, 7] using data sets with simulated movement. The estimation of this effect shows the likely scale of this contribution to an fMRI signal. We have found no paper which attempts to quantify directly the affect on the computed correlation measures.

The purpose of this work is to test whether rigid body co-registration will successfully remove motion effects to an in typical situations to a statistically acceptable level. In this paper we first review the statistical characteristics of published analysis techniques in order to design a test for the effectiveness of rigid-body co-registration which is applicable to the range of current approaches. We then go on to demonstrate the effects of motion and co-registration on the common statistical correlation forms used for analysis.

3 Background

The Blood Oxygen Level Dependent (BOLD) technique relies on the variation in MRI signal due to the physical process of changing proportions of de-oxyhaemaglobin in the blood. Many data sets are generally needed to observe this process, as the signal is of the same order of magnitude as the noise in an individual image. Though the technique does not require injection of a contrast agent it does generally require a relatively restrictive 'on' 'off' paradigm in order to generate data sets during known functional activity/inactivity. In comparison to other functional measurement techniques (such as PET) this method does not provide any direct measurement of quantitative flow. However, BOLD signal is expected to be related to the regional changes in brain activity in areas at least close to the observed signal. The technique is becoming increasingly popular as a clinical as well as a research tool to probe the workings of the brain. However, BOLD is not the only physical mechanism which can lead to a signal change. There are also Blood Flow Level Dependent (b-FOLD), CSF Oxygen Level Dependant (COLD), CSF Flow Level Dependant (c-FOLD) and also motion Level Dependent (MOLD) signal mechanisms [9]. The b-FOLD signal can be considered as complementary to the BOLD signal as an alternative indicator of functional activation. The CSF related signal is not expected to correlate with the stimulus paradigm due to the much shorter time scales. Therefore, the main problem with ensuring valid signal from a BOLD analysis is in controlling the effects of motion, which can be considerable during the course of an extended experiment and often correlate directly with the paradigm task.

There have been many approaches to the analysis of functional NMR images proposed in the literature. Considered from a statistical point of view these techniques can be grouped as either non-parametric or parametric. It is generally accepted that whilst non-parametric techniques are initially more robust, parametric techniques will ultimately have better discriminability once the analytical models have been refined. We therefore concentrate on these approaches here.

For parametric approaches, analysis can be basically decomposed into two stages, the application of a voxel by voxel time dependent analysis, followed by a regional analysis of clusters [8, 11]. The first of these is designed as a significance test, the hypothesis being that the data seen in the image can be accounted

for entirely by random noise fluctuations. The second is a significance test based on the probability of observing particular sizes of regions which fail the first hypothesis. This latter test must take some account of the spatial correlations within images and this is generally done by defining a characteristic smoothing function (such as a Gaussian field) to describe the combined correlation effects of all image formation processes.

The voxel based null hypothesis test is generally implemented as a correlation measure. The details of this vary in the literature, but all successful measures have the same fundamental statistical origins, which is effectively that some measure of correlation C is normalised by it's expected variance $var(C)$ in order to produce a measure which can be treated like a 't test' or 'Z score' [11]. The subsequent thresholding of this measure, to detect significant signals, invariably assumes a Gaussian distribution [1] for this test statistic and must generally take into account temporal correlations in the image formation process [16]. The empirical estimate of variance can be on a voxel by voxel basis or pooled from selected regions of the image. Clearly, if the image formation process does result in uniform random noise across the image then a pooled variance is appropriate and will result in a more stable test statistic. Generally however, this is may not be a reliable assumption for most scanners.

The specific choice of correlation measure varies depending on the authors. Some have suggested using a set of sinusoidal correlation functions and computing the effective "power" of the data [5]. There seem to be two main justifications for this approach, the first is that although the stimulus in the experiment is invariably a simple "on" or "off" task (i.e. a box car function of known period), we do not know the true shape or phase of the signal. Such a Fourier approach to analysis thus gives a method of estimating signal content which is independent of phase or specific details of the shape of the response curve. The second justification is simply that such an approach delivers measures which are completely independent of phase.

A simpler analysis than a Fourier decomposition, involves correlation with a "box car" function [2] which can be shifted as necessary in order to locate the maximum phase response. Though this second technique does not take variability of shape into account there may be some merit in restricting the freedom of the response function to something resembling the initial stimulus. As we do not know the true shape of the signal we are looking for, it would be difficult to know which of these two approaches is superior. However, in general the "box car" approach will be more specific as it requires not only a signal, but a signal with a particular shape. One can attempt to make the method less specific by searching across phases, but any phase shifted correlation or Fourier based analysis should take into account the preferential positive bias in the resulting measures. One model, which has been justified empirically, is a convolution of the stimulus function with the Poisson distribution. This can be generalized to the Gamma variate which is also a popular choice for perfusion analysis [3]. This association may be more than just coincidence if a major contribution to the BOLD signal is actually due to perfusion. If this is true then this would clearly be the most effective way of detecting simple responses.

Another simple variant is to construct pooled estimates of signal from "off" and "on" periods and then to apply a simple "t" test [13]. Simple algebra can show that this is statistically equivalent to correlation with a "box car" function. Clearly such an approach does not take correct account of either temporal correlations or the specific shape of the response curve.

Finally, some authors have suggested correlation measures which cannot be directly interpreted as a 't-test'. The measure used both in [1] and [12] in particular is a measure which occurs in the STIMULATE software which is commonly used in research laboratories. Though this has nice intuitive properties (it is normalised between -1 and 1) it cannot be reliably thresholded in order to identify true signal as the measure has different statistical scaling for each experimental design. This matter will be discussed further below. In [4] the test statistic is defined as a power-quotient which is the power of the sought frequencies divided by a normalisation factor other than the expected variance. This particular form of measure is only monotonically related to the standard form described above. However, before this

[1] This can ultimately be justified by the central limit theorem if the variance of the correlation measure is the combined affect of many small purtebations in the image data drawn from unknown but equal distributions.

measure is used it is renormalised using a Monte-Carlo technique to re-impose the standard statistical interpretation. A similar step would also be necessary with the measure in [1] and [12] before it could be used in earnest. In doing so this would be reverting to the previous measures.

4 Methods

Experimental Design

Experiments were performed on 6 healthy volunteers (5 men, 1 woman; mean age 26.8 years, range 19-34). 5 were right handed and 1 left-handed by self-report. To minimise head movements foam padding and a velcro strap were used to secure the head. A bite bar with a groove was used to provide a reference for subjects to rest their front teeth upon in order to minimise out of plane movements during scanning. All volunteers gave informed written consent after the nature of the experiment had been fully explained.

All fMRI experiments were performed on a Phillips Gyroscan ACS NT 1.5T system. Each subject was positioned supine inside the MR scanner. Imaging consisted of 18 dynamic acquisitions of 50x3 mm contiguous transverse slices covering the whole head. The imaging protocol consisted of a T2*-weighted gradient echo sequence with multi-shot echo planar collection (TR= 250 ms, TE= 40 ms, Flip Angle = 40 ^{o}, EPI factor 5, matrix 128x128, FOV of 200 mm^2).

Image acquisition was 1 minute 14 seconds per 50-slice volume. A functional imaging sequence consisted of 18 sequentially acquired multislice images. Volunteers A-C were scanned at rest. Subjects were instructed to lie still during the acquisition of the image sequence. In volunteers D-F a motor activation paradigm was performed during scanning. The task consisted of opposing each finger to the thumb in turn (in the order 2, 3, 4, 5, 5, 4, 3, 2). Finger opposition was self-paced using the dominant hand. Subjects briefly practiced this task prior to entering the scanner to ensure that they knew what was expected of them during the activation periods. Movements were performed with 3 scans during activation alternated with three scans at rest. The cycle was repeated 3 times with a total data acquisition time of 22 minutes and 12 seconds. Our MRI sequence is very similar to those which are commonly used in fMRI BOLD experiments, though we have worked with entire brain volumes and extended the time of data aquisition to be slightly longer than would be used on average so that we can improve our statistics and observe the effects of motion and subsequent correction more completely.

Data analysis was performed on a SUN SPARC station 20 (unix workstation) running Solaris 2.4. For each subject slice 32 of 50 from the original, motion corrected and synthetic data sets were extracted for statistical analysis. Analysis was performed using our own C software developed using the TINA machine vision and image analysis environment [19]. Resliced datasets were produced using a 5x5x5 windowed renormalised sinc interpolation algorithm [15].

In this paper we have also included one data set from an fMRI visual activation study to illustrate the use of the developed techniques as a quality control mechanism. Imaging consisted of 18 dynamic acquisitions of 50x3 mm contiguous transverse slices covering the whole head. The imaging protocol consisted of a T2*-weighted gradient echo sequence with multi-shot echo planar collection (TR= 250 ms, TE= 40 ms, Flip Angle = 40 ^{o}, EPI factor 5, matrix 128x128, FOV of 200 mm^2). Image acquisition was 1 minute 14 seconds per 50-slice volume. A functional imaging sequence consisted of 81 sequentially acquired multislice images. THIS IS WRONG EMMA?

Analysis Methods

The various approaches to fMRI data analysis vary in detail but the substance of the approach has common origins. Though the ability to extract signal will be strongly dependent on having the correct functional form and phase, the technique of error propagation can be used to show that any normalised wave-function will produce a set of correlation measures with an identical distribution for the null hypothesis. We thus choose to work with a square wave for simplicity. The particular choice of correlation

measure, however, can make a difference to the behavior of the background data under the null hypothesis. In particular a t-test like approach will behave differently to the normalised measure used in STIMULATE [1]. The effects of motion artefacts on both of these measures thus need to be investigated. The three measures, chosen to cover a set of statisically distinct possible approaches, were used for this investigation;

- A simple correlation measure with no explicit (fixed) normalisation.

$$C_j^1 \;=\; \sum_{t=1}^{T} I_{tj}.W_t$$

  where W is a normalised correlation waveform ($|W|^2 = 1$) and I_j is a mean subtracted temporal data set at voxel j . This correlation measure can be converted into a simple null hypothesis statistic by dividing by a pooled estimate of the standard deviation on the measure $\sqrt{var(C)}$ and will behave in the same way as any measure which makes the basic assumption of constant uniform image noise, including Fourier approaches. While we accept that such a simple measure is unlikely to be used unmodified in serious fmri analysis we have included it here for completeness.

- A correlation measure with individual voxel based normalisation.

$$C_j^2 \;=\; \frac{\sum_{t=1}^{T} I_{tj}.W_t}{1/(T-1)\sqrt{\sum_t^T (I_{tj} - W_t.C_j^1)^2}}$$

  where the numerator is the estimate of variation about the assumed model. Once again I_j is a mean subtracted temporal data set at voxel j . This technique will behave in the same way as any measure which estimates variance from the data, such as 't-tests' and 'z-scores'.

- and finally a normalised correlation measure as used in STIMULATE

$$C_j^3 \;=\; \frac{\sum_{t=1}^{T} I_{tj}.W_t}{\sqrt{\sum_t^T I_{tj}^2}}$$

  with parameters as described above. This measure is nicely normalised between -1 and 1 but cannot be interpreted as a standard null hypothesis statistic unless the numerator approaches that of C_j^2, which will only happen when the noise dominates the observed signal distribution (i.e. C_j^1 is small).

Correction of data correlation either by a Bonferroni factor or other, will modify only the interpretation of the estimated correlation values. It will not significantly modify the resulting correlation measures available for interpretation. Similarly any latter stages of group statistical significance analysis cannot correct for errors already introduced by the voxel based correlation measure. Thus by working with raw (non-thresholded) data we may be able to demonstrate the direct effects of motion artefacts on any correlation based analysis.

The effects of motion on correlation scores can be analysed as a series of steps. Any induced motion effects grey level values locally and these changes then feed through to the numerator and denominator terms of the correlation measures. For locally continuous image structure and small motions (of the order of pixel size) the local image structure can be approximated by an average value and an oriented gradient. This first order model predicts that the effects of motion on the grey level values will be proportional to the local image gradient. The effects of an unknown motion on the final correlation measures may be quite unpredictable, but if the motion is correlated with the stimulus then there will be systematic changes in correlation measures which must be proportional to local image gradient. Areas of the image which contain no structure (i.e. zero gradient) cannot be affected by motion. If the motion is uncorrelated with the stimulus then there will be an increase in correlation variance (i.e. reduction is correlation stability). This effect will again be proportional to the local image gradient. It is these effects which we would like to remove by motion correction.

Experimental Process

Our investigation involves the following steps.

- Calculate rigid body motion for genuine null hypothesis data (no activation) for two groups of three subjects. One group performing the motion stimulus paradigm and the others at rest. All data were registered to a base volume for each volunteer using the Woods algorithm [17, 18]. The main automated image registration (AIR) parameters were set as follows: intensity threshold = 275, initial sampling interval = 81, final sampling interval = 1 pixel, sample increment decrement ratio = 3, convergence criteria = 0.0005, maximum number of iterations for each sampling density = 300, no spatial smoothing was used, interpolation to standard voxel size was active.

- Compute simulated data from the motion vectors.

  The motion parameters were used to interpolate a set of data from the first volume with equivalent motion vectors to those estimated by the AIR package.

- Demonstrate the effects of motion on the correlation measures used in real data.

  As the effects of motion are expected to be proportional to local image gradient, we plot correlation scores against this quantity. Here we define image gradient G_j as follows;

$$
\begin{aligned}
dI_{x,y}/dx &= (I'_{x+1} - I'_{x-1})/2 \\
dI_{x,y}/dy &= (I'_{y+1} - I'_{y-1})/2 \\
G_j &= \sqrt{((dI_j/dx)^2 + (dI_j/dy)^2)}
\end{aligned}
$$

  where x and y are image indices and I' is the first input image of the temporal sequence smoothed with a unit Gaussian kernel. The smoothing process sets the scale for the range of applicability of the linear assumption and allows the gradient information to be estimated from a single temporal slice. Averaging of the temporal data set to produce a mean gradient would also be possible and perhaps even preferable for very large motions, but was not found necessary for this work.

  For data without motion artefact, this plot is expected to show the correlation score , distributed normally around zero correlation with variable density along the image gradient axis. For this case a fixed threshold value will have the same affect in terms of rejecting the null hypothesis for all values of image gradient. Any variation from this distribution shows itself as increased broadening or non-ideal structure perpendicular to the image gradient axis.

- Demonstrate that these effects are also visible in the simulated data.

  The simulated data, being effectively noise free, does not yield sensible variance estimates in the denominator terms of the standard correlation measures, C^2 & C^3. However, the individual estimates of the denominators are expected to be quite constant across the dataset. As a consequence C^1 is used to analyse the simulated data as it is expected to behave in a very similar fashion to the other two measures.

- Demonstrate that these effects are removed by rigid body co-registration in the real data by repeating the analysis for motion corrected data.

- Finally, simulate the effect of isolated failiures of coregistration by shifting an image in each coregistered sequence.

5 Results and Discussion

As explained above, we expect motion artifact to be statistically proportional to the local gradient in the image. This is the effect of motion feeding directly through into the computed scores. We can therefore investigate the degree of motion artefact by plotting correlation score against image gradient. The scatter plots produced are 'self calibrating'; the axis scaling of the plots is implicitly defined. The effects of motion are expected to be negligible for small image gradient so the distribution of data in this region can be used to infer a probablility level for the null hypothesis for all of our correlation measures. In particular the outer limits of this part of the distribution correspond to a probability value of 2.0 e-5 (i.e. one part in a 200x256 image). They can be visually interpreted for all correlation measures, without the need for correlation score or edge gradient axes, which are scaled differently by the level of MR image noise and paradigm design (number of measurements) for each correlation method.

	Pitch	Roll	Yaw	X	Y	Z
A	0.20 ^{o}	0.22 ^{o}	0.30 ^{o}	0.49 pixels	0.31 pixels	0.06 pixels
B	0.22 ^{o}	0.49 ^{o}	0.16 ^{o}	0.25 pixels	0.50 pixels	0.11 pixels
C	0.22 ^{o}	0.33 ^{o}	0.18 ^{o}	0.28 pixels	0.30 pixels	0.09 pixels
D	0.90 ^{o}	0.60 ^{o}	0.38 ^{o}	0.96 pixels	0.84 pixels	0.31 pixels
E	0.85 ^{o}	0.06 ^{o}	0.41 ^{o}	0.45 pixels	0.57 pixels	0.16 pixels
F	0.39 ^{o}	0.12 ^{o}	0.37 ^{o}	0.37 pixels	0.41 pixels	0.17 pixels

Table 1 Standard deviations on estimated movement for each subject calculated using AIR

Our results for the standard deviations on the estimated motion are shown in Table 1 for the two groups of three subjects (A,B,C and D,E,F). For the group with no stimulus these results are close to the expected accuracy of the AIR software (i.e. R.M.S. error of less than a pixel anywhere in the image). The motion scatter plots (Figure 1) show no unexpected structure and there is no observable correlation between edge contrast and the correlation score for any of the three measures. These results effectively represent the ideal result we would like to achieve after motion correction.

The second experiment with three subjects (D,E,F) performing a simple motor task show significant movement (Table 1) which is consistent with R.M.S. errors of a few pixels and generates plots with distinct structure, figure 2. Notice the broadening of the data in the y-dimension (correlation score) towards the end of the x-axis where the image gradient is largest (at edges). This structure is regenerated up to the level of random noise by applying motion vectors estimated using the AIR software to the genuine null hypothesis data (no activation), figure 3. The distributions we see in these plots are entirely consistent with rigid body motion plus random noise. In contrast the plots of correlation scores for co-registered data against the same edge contrast measures, figure 4, show that this correlation has been significantly reduced by the process of coregistration. In this data the first correlation score C^1 shows a gradual increasing instability (broadening) of the correlation score with edge contrast. This is reduced using correlation score C^2 which explicitly estimates the variance from the sample data and does not assume constant uniform variance on the underlying data set.

It is also interesting to note that the measure C^3 is marginally less affected by motion than the conventional null hypothesis statistic. This is because the denominator term (which is a good approximation to the noise level for small signal) is increased by the variation in the image data induced by motion. At first sight this measure would seem to be more robust to these effects. It may be just such robustness combined with simplicity of use which has maintained the popularity of this approach in the literature [14]. However, while this may be adequate for visually identifying relative large measures, the lack of a meaningful scaling makes this correlation score difficult to interpret in an absolute sense. This functional form is expected to be less specific in it's response to signal.

We began this work aiming to determine whether the rigid body assumption is an adequate model for motion correction in fMRI analysis and we are now in a position to answer this question. The main

problem with motion artefacts is that they may mimic the effects of signal by correlating directly with the stimulus response function. This has indeed been shown to be an effect in real data (figure 2). A secondary effect is the decrease in stability of the observed data values. No motion correction proceedure can be perfectly accurate and some residual errors are to be expected. This can be observed after motion correction by calculating the ratio of variances for the correlation measures for two ranges of image gradient, see table 2. The ratio of the variance is calculated between the first and second eighth of the dynamic range of image gradients (x-axis). This lower region of the plot is within brain tissue (the second eighth of the data corresponds to the boundary between brain tissues) and thus is within the expected fMRI signal area. Results are less stable around the skull boundaries due to the very high image gradients involved, but this region of the data is less important to fMRI analysis. The accuracy of these ratio is of the order of 1%. Table 2 shows that C^1 in particular is badly affected by the increased instability around edges. This is not such an issue for correlation measures which estimate the variance from the data (in particular C^2).

Subject	D	E	F
C^1	1.27	1.21	1.13
C^2	1.00	0.98	1.05
C^3	1.01	1.03	1.04

Table 2 Dimensionless measures of relative standard deviation for intermediate and low gradient correlations $\sqrt{var(C_{1/8})/var(C_{0/8})}$.

When performing rigid body alignment with an automated system there is always a chance that the alignment algorithm will fail. This cannot be avoided as all iterative optimisation routines have potential problems with local minima. When this happens (if it is not picked up by a validation process) it will generate isolated temporal data points at each voxel which are effectively outliers. These data points will cause a change in the computed correlation which will reduce the overall correlation scores for measures such as C^2. This is because the linear variation in the numerator will always be smaller than the quadratic change in the denominator. We can illustrate this by offsetting the first image in each sequence of data by two pixels and recomputing the variances for gradients corresponding to tissue boundaries, table 3.

Subject	D	E	F
C^1	1.31	1.58	1.21
C^2	0.96	0.99	0.93
C^3	0.96	0.98	0.95

Table 3 Dimesionless measures of relative standard deviation of intermediate gradient correlations for shifted data $\sqrt{var(C_{1/8})/var(C_{0/8})}$.

In general, any motion correction technique, even a poor one, removing the majority of the motion from the data set and leaving only residual behaviour which is uncorrelated with the stimulus response curve, will not invalidate (statistically) the conclusions of any study using such a measure. This is an important result, as a poor motion correction procedure will result in less confidence in the observed outcome, it would be difficult to generate an erroneous positive results from an experiment due to motion artefacts. Our results suggest that rigid body coregistration does effectively remove false correlations caused by motion correlated to the stimulus response.

6 Use of Motion Correlation PLots in fMRI Quality Control

We have been using the new motion correlation scatter plots as a method of assessing quality of data emerging from our analysis chain. We illustrate their use here with the results from one analysis during

the detection of a BOLD response to a visual stimulus. Figure 5(a) shows a motion correlation plot for data generated during analysis (C^2). Activations are present in this data at both high and low level image gradient. In itself this would not be unduly worrying, but there is also a general broadening of the underlying distribution for positive correlation values at high gradient. On closer inspection this data set was found to have systematic shift artefacts at the level of 0.5 pixels in almost half of the re-sliced data set due to failiure of the automatic co-registration software. The region of relatively unambiguous activation is shown as a rectangle. The new analysis technique allowed us not only to identify genuine activation (Figure 5(b)), but also perform quality control on our software analysis chain.

7 Conclusions

We have analysed the affect of motion on fMRI analysis. Given the broad range of approaches in the literature we have concentrated this analysis on the common statistical foundations of the parametric methods, which are the use of correlation measures. Our results are expected to be independent of the details of the shape of the correlation stimulus and should generalise to all fMRI studies based on assessing levels of significance from correlation scores.

We have constructed a method for visualising the effects of motion on fMRI analysis. As the effects of motion are expected to be proportional to the local image gradient, a scatter plot of correlation function versus image gradient separates the effects of motion across the plot. This distribution is self scaling, easily visually interpreted and can be used as a general tool to check the relative accuracy of different motion correction proceedures. Such a method could also be used with non-normalised correlation measures (ie C^1) in order to assess the adequacy of particular coregistration proceedures in the absence of ground truth.

In this study we have used the new technique to visualise the effects of motion in a typical fMRI study for three correlation approaches. The results indicate that motion artefacts are manifest in motion based experiments. These effects are significantly reduced after motion correction but still observable in simple correlation analyses which assumed pooled variance. Finally, null hypothesis based correlation methods which estimate the variance from the data at each voxel are unaffected by motion provided that any resulting residual motion, is uncorrelated with the stimulus. On this basis, as we see no residual correlation with the stimulus response curve following rigid body re-alignment, we consider the rigid body assumption an acceptable basis for motion correction for these measures. In general, it will never be possible to remove all stimulus correlated motion completely, but techniques, such as those described here, could be used to monitor the success or failiure of attempts to do so.

References

1. Bandettini P, Jesmanowicz A, Wong E C, Hyde J S., **Processing Strategies for Time Course Data Sets in Functional MRI of the Human Brain**, M.R.M, 30, 161-173, 1993.
2. Baudendistel K, Schad L R, Friedlinger M, Wenz F, Schroder J and Lorenz W J., **Post-Processing of Functional MRI data of Motor Cortex Stimulation Measured with a Standard 1.5 T Imager**, M.R.I, 13, 701-707,1995.
3. Benner T, Heiland S, ERB G, Forsting M and Sartor K, **Accuracy of Gamma-Variate Fits to Concentration-Time Curves from Dynamic Susceptibility-Contrast Enhanced MRI: Influence of Time Resolution, Maximum Signal Drop and Signal-to-noise**, M.R.I., 15(30, 307-317 , 1997.
4. Brammer M L, Bullmore E T, Simmons A, Williams S C R, Grasby P M, Howard R J, Woodruff P W R, and Rabe-Hesketh S. **Generic Brain Activation Mapping in Functional Magnetic Resonance Imaging: A Non-Parametric Approach**, M.R.I., 15, 763-770, 1997.
5. Bullmore E, Brammer M, Williams S C R, Rabe - Hesketh S, Janot N, David A, J.Mellers, R.Howard, P.Sham., **Statistical Methods of Estimation and Inference for Functional MR Image Analysis**, M.R.M., 35, 261-277, 1996.
6. Friston K J, Williams S, Howard R, Frackowiack R S J, and Turner R, **Movement-Related Effects in fMRI Time-Series**, M.R.M., 35, 346-355, 1996.
7. Friston K J, Ashbuner J, Frith C D, Poline J B, Heather J D, Frackowiak R S J, **Spatial Registration and Renormalisation of Images**, M.R.M., 2, 165-188 1995.
8. Friston K J, Holmes A, Poline J-B, Price C J, Frith C D, **Detecting Activations in PET and fMRI: Levels of Inference and Power** Neuroimage, 40, 223-235, 1996.
9. Hajnal J V, Young I R and Bydder G M, **Contrast Mechanisms in Functional MRI of the Brain**, Advanced MR Imaging Techniques, Ed's W. G. Bradley Jr and G. M. Bydder, Martin Dunitz Ltd London, 195-207, 1997.
10. Jiang A, et. al. **Motion Detection and Correction in Functional MR Imaging** H.B.M., 3, 224-235, 1995.
11. Lange N., **Tutorial in Biostatistics, Statistical Approaches to Human Brain Mapping by Functional Magnetic Resonance Imaging**, Statistics in Medicine, 15, 389-428, 1996.
12. Presciutti O, Pelliccioli G P, Tarducci R, Chiarini P and Gobbi G., **New Processing Methods in Functional MRI**, Rivista di Neuroradiologica, 10, 261-264, 1997.
13. Sadato M, Ibanez V, Deiber M, Campbell G, Leonardo M and Hallet M., **Frequency Dependant Changes of Regional Cerebral Blood Flow during Finger Movement**, Journal of Cerebral Blood Flow + Metabolism, 16,23-33, 1996.
14. Strupp, J P, **Stimulate: A GUI Based fMRI Analysis Software Package** Neuroimage, 3, 1996.
15. Thacker N A, Jackson A, Moriarty D and Vokurka B, **Renormalised SINC Interpolation**, proc. MIUA, pp33-36 Leeds, July 1998.
16. VanGelderen P, Ramsey N F, Liu G, Duyn J H, Frank J A, Weinberger D R and Moonen C T W, **Three-Dimesional Functional Magnetic Resonance Imaging of Human brain on a clinical 1.5 T Scanner**, Proc. Nat.Ac.Sci, USA, 92, 6906-6910, 1995.
17. Woods R P, Cherry S R and Mazziotta J C, **Rapid Automated Algorithm for Aligning and Reslicing PET Images**, JCAT. 16, 620-633, 1992.
18. Woods R P, Mazziotta J C and Cherry S R , **MRI-PET Registration with an Automated Algorithm**, JCAT, 17, 536-546, 1993.
19. **URL:** www.niac.man.ac.uk/Tina.html

Figures

- Figure 1. Correlation scores vs. edge contrast (G). (no Stimulus)
- Figure 2. Correlation scores vs edge contrast (G). (Stimulus)
- Figure 3. Correlation scores vs edge contrast (G). (Response from simulated data)
- Figure 4. Correlation scores vs edge contrast (G). (Stimulus response after motion correction).
- Figure 5. Quality control for fMRI data analysis using Correlation scores vs. edge contrast (G).

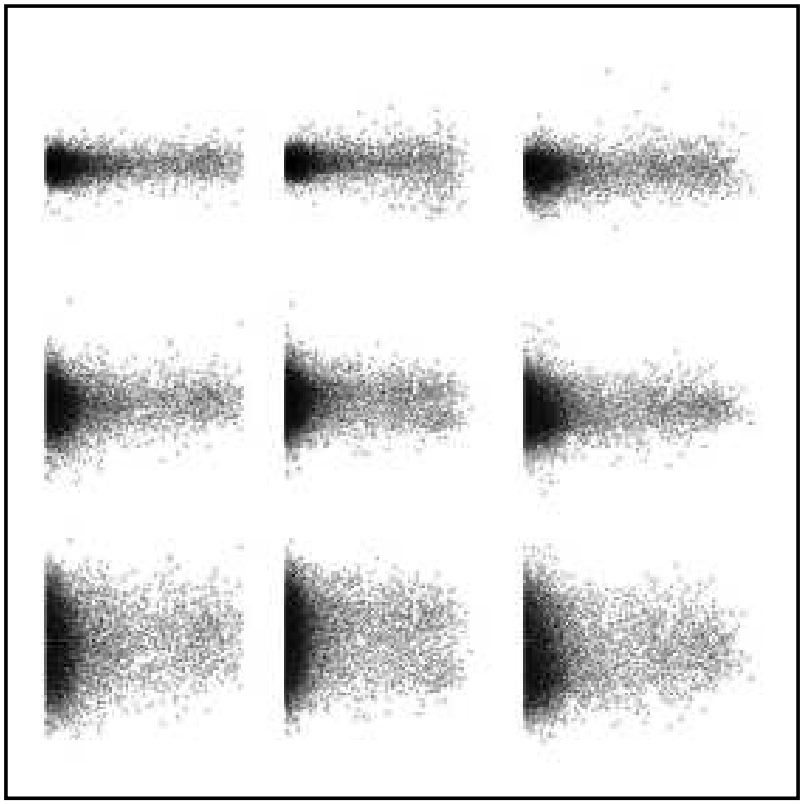

Figure 1: Correlation scores vs. edge contrast (G). No stimulus condition for subjects A, B and C (columns), and correlation scores C^1, C^2, C^3 (rows).

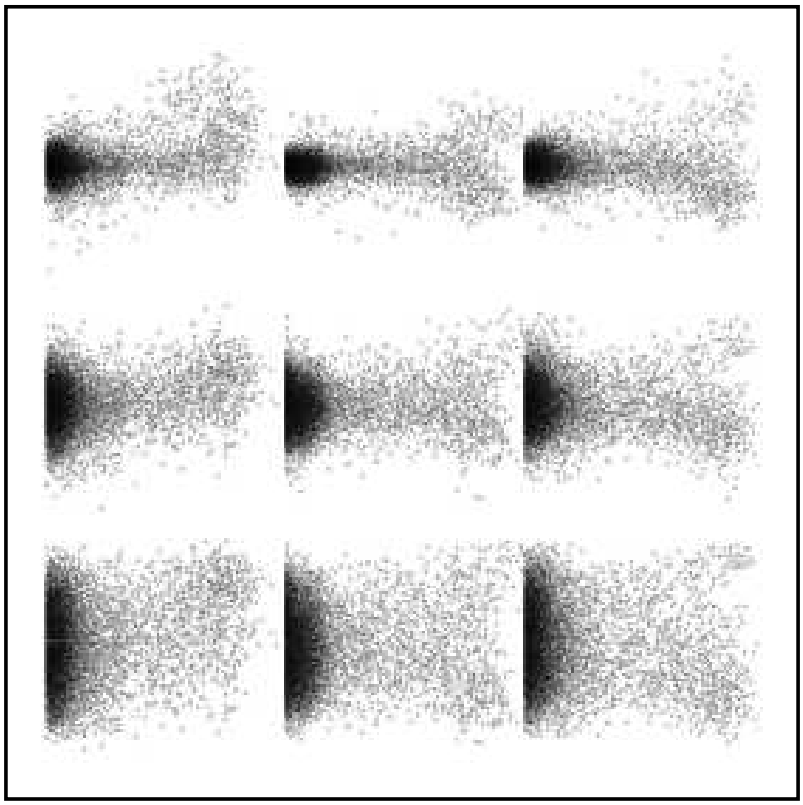

Figure 2: Correlation scores vs edge contrast (G). Motion stimulus condition for subjects D, E and F (columns), and correlation scores C^1, C^2, C^3 (rows).

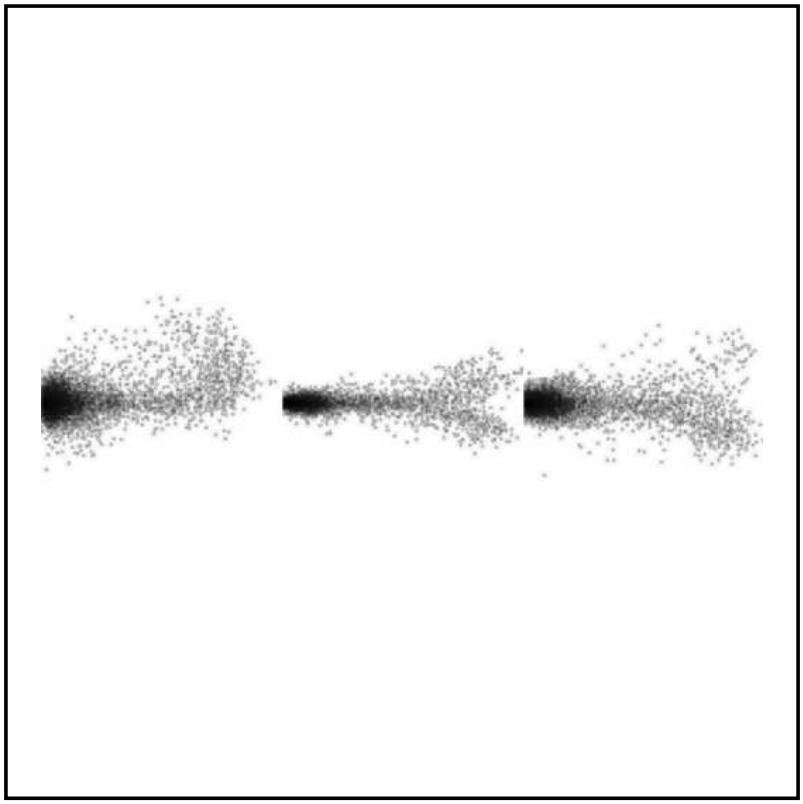

Figure 3: Correlation scores vs edge contrast (G). Simulated stimulus for subjects D, E and F correlation C^1.

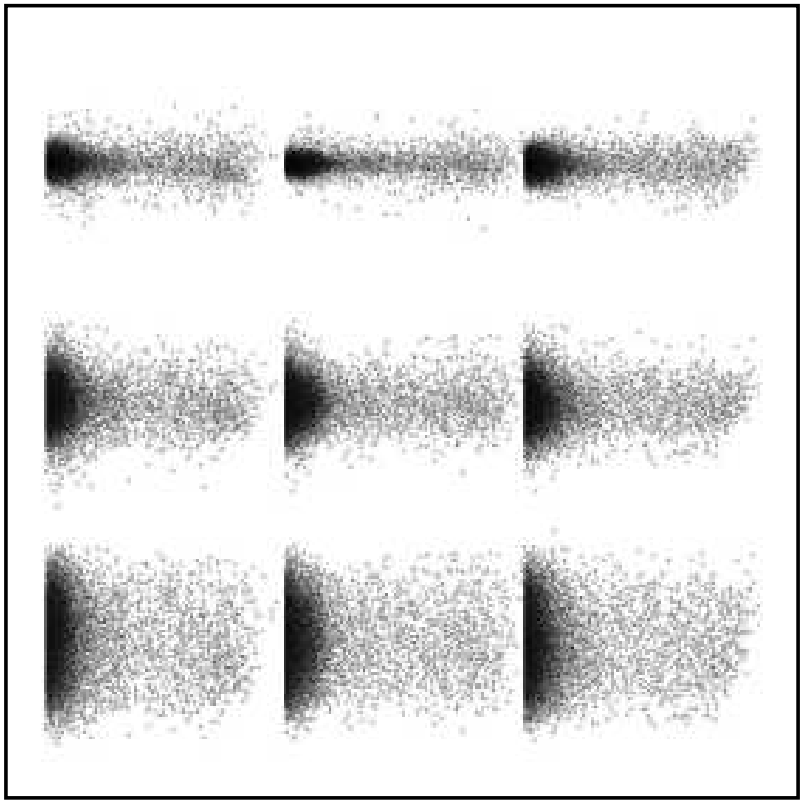

Figure 4: Correlation scores vs. edge contrast (G). Motion corrected stimulus for subjects D, E and F (columns), and correlation scores C^1, C^2, C^3 (rows).

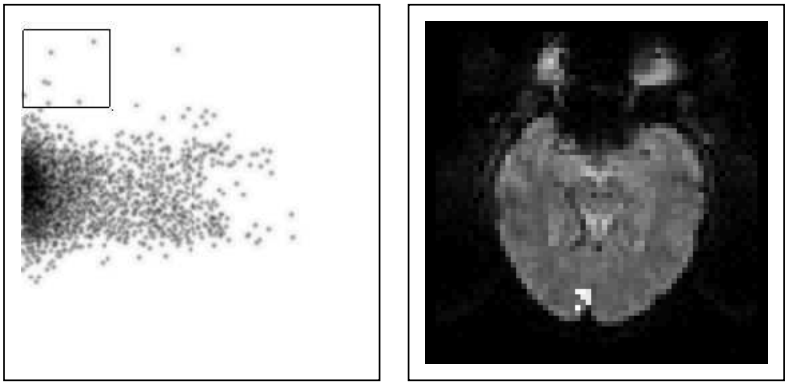

(a) Correlation score C^2 vs edge contrast

(b) fMRI image with superimposed activation

Figure 5: Quality Control of fMRI Analysis showing the activation corresponding to unambiguous correlations (data within manually selected box)